Med Microbiol Immunol (2015) 204:215–226
DOI 10.1007/s00430-014-0357-y

ORIGINAL INVESTIGATION

Pfs promotes autolysis-dependent release of eDNA and biofilm formation in *Staphylococcus aureus*

Yan Bao · Xu Zhang · Qiu Jiang · Ting Xue · Baolin Sun

Received: 2 July 2014 / Accepted: 26 August 2014 / Published online: 4 September 2014

Abstract *Staphylococcus aureus* is a major biofilm-forming pathogen, and biofilm formation remains an obstacle in the treatment of clinical *S. aureus* infection. Methylthioadenosine/S-adenosylhomocysteine nucleosidase (Pfs) has been implicated in methylation reactions, polyamine synthesis, vitamin synthesis, and quorum-sensing pathways. In this study, we observed that the deletion of *pfs* gene in *S. aureus* NCTC8325 reduced bacterial clumping ability and resulted in the decreased biofilm formation under both static and dynamic flow conditions in an autoinducer-2-independent manner. While the PIA amount was not affected, the *pfs* mutation significantly decreased the amount of eDNA present in the biofilm and the cell autolysis. Consistent with reduced autolysis, the transcription levels of the autolysin genes, *lytM* and *atlE,* were reduced in the absence of Pfs. These data suggest that Pfs promotes autolysis-dependent release of eDNA and biofilm formation in *S. aureus*, and our findings indicate that Pfs is a potential novel target for anti-biofilm therapy.

Yan Bao and Xu Zhang have contributed equally to this work.

Electronic supplementary material The online version of this article (doi:10.1007/s00430-014-0357-y) contains supplementary material, which is available to authorized users.

Y. Bao · X. Zhang · Q. Jiang · B. Sun (✉)
Department of Microbiology and Immunology, School of Life Sciences, University of Science and Technology of China, Hefei 230027, Anhui, China
e-mail: sunb@ustc.edu.cn

T. Xue
School of Life Science, Anhui Agricultural University, Hefei 230036, Anhui, China

Keywords *Staphylococcus aureus* · *pfs* · Biofilm · Autolysis · eDNA

Introduction

Staphylococcus aureus is widely present in both natural and clinical environments, with approximately one-third of the human population carrying this bacterium [1]. *S. aureus* is a major cause of infectious morbidity and mortality in both community and hospital settings [2, 3]. Many *S. aureus* infections involve the formation of biofilm, comprising surface-associated communities of microbes within an extracellular matrix [4]. The ability to form biofilm is an important aspect of *S. aureus* pathogenesis [5]. Bacteria within the biofilm exhibit social behaviors analogous to those observed in higher organisms, as these microbes communicate and rapidly adapt to changing growth environments [6, 7]. The extracellular matrix of the biofilm creates a structural barrier, provides a physiological niche, and protects bacteria from harsh environmental conditions, including the host immune response and antibacterial agents [8–10]. The formation of these sessile communities and their inherent resistance to antibiotics and host immune attack underlie many persistent and chronic bacterial infections [11, 12].

Bacterial biofilm formation proceeds in two steps: the initial adhesion of bacterial cells onto biotic or abiotic surface, followed by cell proliferation and the secretion of an extracellular matrix that contributes to intercellular aggregation [13]. The biofilm matrix of *S. aureus* primarily comprises polysaccharides, proteins, and extracellular DNA (eDNA) [14], but the composition of individual biofilms varies among different strains and is dependent on the metabolic state and growth conditions [15].

Table 1 Plasmids and bacterial strains used in this study

Strains of *S. aureus*	Relevant genotype	Reference or source
WT	NCTC8325 Wild type	NARSA
SBY1	8325 *pfs*::*ermB*	[23]
SBY2	8325 pLI50	[23]
SBY3	8325 *pfs*::*ermB* pLI50	[23]
SBY4	8325 *pfs*::*ermB* pLIpfs	[23]
SBY5	8325 pgfp	[23]
SBY6	8325 *pfs*::*ermB* pgfp	[23]
RN6911-pLI50	RN6911 pLI50	This study
RN6911-*pfs* mutant	RN6911 *pfs*::*ermB* pLI50	This study
RN6911-*pfs* C	RN6911 *pfs*::*ermB* pLIpfs	This study
SH1000-pLI50	SH1000 pLI50	This study
SH1000-*pfs* mutant	SH1000 *pfs*::*ermB* pLI50	This study
SH1000-*pfs* C	SH1000 *pfs*::*ermB* pLIpfs	This study
Plasmids		
PLI50	Shuttle cloning vector, Ap^r Cm^r	Addgene
pLIpfs	pLI50 with *pfs* and its promoter, Ap^r, Cm^r	[23]
pBTpfs	Plasmid derivative from pBT2 for *pfs* deletion	[23]

NARSA Network on Antimicrobial Resistance in *Staphylococcus aureus*

Extracellular DNA serves as an adhesive and strengthens biofilms [16]. Cell lysis is a major source of eDNA in biofilms, and the genes associated with autolysis have been implicated in *S. aureus* biofilm formation [14, 17]. The major autolysin genes of *S. aureus* include *atlE*, *lytM*, *lytH*, *lytA*, *sle1,* and *lytN* [18]. In addition, the genes involved in autolysis also include *lrgAB*, which inhibit autolysis, and *cidAB*, which induce cell lysis. Autolysis is generally tightly regulated, and many regulatory loci have been implicated in the regulation of autolysis in *S. aureus*, including negative regulators, such as ArlRS, MgrA, LytSR, SarA, and SarV, and the positive regulator, *agr* quorum-sensing system [18].

As an important part of the S-adenosylmethionine (SAM) cycle, methylthioadenosine/S-adenosylhomocysteine nucleosidase (Pfs) function in a broad array of metabolic reactions, such as methylation reactions; the recycling pathway of adenine, sulfur, and methionine; and the synthesis of polyamine, vitamin, and the universal quorum-sensing signal, autoinducer-2 (AI-2) [19, 20]. It has been reported that Pfs inhibitors disrupt AI-2 production in *Vibrio cholerae* and *Escherichia coli* in a dose-dependent manner without affecting growth and biofilm formation in these organisms [21]. We have previously shown that AI-2 reduces *S. aureus* biofilm formation via the *icaR* activation pathway [22], and Pfs is essential for AI-2 production [23]. The aim of the present study is to investigate the role of Pfs in *S. aureus* biofilm formation. The biofilm formation of the *pfs* mutant strain was compared with that of the isogenic wild-type strain. We observed that the *pfs* mutation reduced *S. aureus* biofilm formation, which is associated with reduced autolysis and eDNA levels in the biofilm.

Materials and methods

Bacterial strains and growth conditions

The phenotypic and genotypic properties of the *S. aureus* strains used in this study are listed in Table 1. All *S. aureus* strains were grown in tryptic soy broth (TSB) containing 0.25 % glucose (Difco, Detroit, MI, US) at 37 °C with shaking, unless otherwise stated. When required, the media were supplemented with 15 μg/ml of chloramphenicol.

Deletion and complementation of the *pfs* gene

The *pfs* mutant strain of *S. aureus* was generated using the plasmid pBTpfs as previously described [23]. The complementation of *pfs* was achieved using the plasmid pLIpfs [23].

Biofilm assay under static conditions

A static biofilm formation assay was performed using the microtiter plate test based on a previously described method [24]. Briefly, cultures incubated overnight in TSB at 37 °C were diluted 200-fold with fresh TSB (containing 0.25 % glucose) supplemented with 3 % NaCl. The diluted cell suspension was inoculated into flat-bottomed 96-well polystyrene plates (Costar 3599), with 200 μl in each well. After incubated at 37 °C for 24 h, the wells were gently rinsed three times with water to remove non-adherent cells and dried using absorbent paper. Subsequently, the wells were stained with 0.5 % crystal violet for 10 min and rinsed again with water to remove any unbound stain. The plates were dried and the absorbance was measured at 560 nm with an enzyme-linked

immunosorbent assay reader in a 3 × 3 scan model. To determine the effect of AI-2, the medium was supplemented with chemically synthesized 4,5-dihydroxy-2,3-pentanedione (DPD), the AI-2 precursor molecule, at a concentration of 39 or 390 nM, at the beginning of incubation. The AI-2 precursor molecule, DPD, of which the storage concentration is 3.9 mM dissolved in water, was purchased from Omm Scientific Inc., TX, USA. To test the impact of DNase I, the cells were grown in medium supplemented with 25 Kuniz units/ml of RNase-free DNase I (Sangon Biotech).

Biofilm assay in the flow cell system

Biofilm formation under flow conditions was determined in disposable flow cells (Stovall Life Science, Greensboro, NC), as previously described [25]. Before each inoculation, the system was primed with culture medium (66 % TSB with 0.165 % glucose), and the flow of the culture medium was stopped. Biofilm formation was initiated after inoculating the flow cell chamber with overnight cultures diluted at 1:100 in the culture medium; a total of 5 ml of the diluted culture was injected into the chamber. The upside of the flow cell was turned down, with the glass surface downwards, to establish the cells on the glass surface of the flow cell and subsequently turned upright after 1 h of incubation at 37 °C. After this incubation period, the culture medium was continually perfused over the flow cell system using a high-precision tubing pump with a planetary drive (ISMATEC, Switzerland) at a rate of 0.5 ml/min. During biofilm development, macroscopic images were taken using a Canon EOS camera with a macroscopic lens (18–55 mm) (Canon Inc, New York, NY). For the confocal laser scanning microscopy (CLSM) analysis, strains with the GFP protein expressed on the plasmid were used (SBY5 and SBY6). Fluorescence images of the biofilm were obtained using CLSM (OLYMPUS FV-1000, BX61WI) confocal microscopy with a 10× OLYMPUS UPLFL object (NA 0.3) and a 20× OLYMPUS UPLFL object (NA 0.46). The fluorescence of the GFP was excited with an argon laser at 488 nm, and the emission band-pass filter used was 515 ± 15 nm. Z-Stacks were collected at 1.0-μm intervals, and the confocal image stacks were constructed using IMARIS 7.0 (Bitplane, Switzerland) for three-dimensional (3D) reconstruction. All confocal parameters were set using the SBY5 biofilm and were used as standard settings for comparing the biofilm produced by SBY6. Regions of interest within the biofilms were selected from similar areas within each flow cell chamber, and each confocal experiment was repeated at least two times.

Bacterial clumping assay

Growth phenotype of overnight cultures incubated at 37 °C in glass tubes in TSB was compared. The clump structure of the log phase cultures was further observed. *S. aureus* cultures were grown at 37 °C in TSB medium, and aliquots of the cultures were removed at various growth phases. The bacterial clumping of the cultures was observed, and the images were obtained using a Nikon TE2000-U inversed microscope.

PIA detection

PIA was detected as previously described [26], with little modification. Briefly, bacterial cells were grown overnight in TSB, and the same number of cells (2 ml) from each culture was resuspended in 50 μl of 0.5 M EDTA, pH 8.0. Cells were then incubated for 5 min at 100 °C and centrifuged to pellet the cells, and 40 μl of the supernatant was incubated with 10 μl of proteinase K (20 mg/ml, Sangon, China) for 30 min at 37 °C. The extracts (2 μl) were spotted on a nitrocellulose membrane, dried, and blocked with 3 % bovine serum albumin. The membrane was then incubated at room temperature for 1 h in PBS containing 0.8 μg/ml wheat germ agglutinin conjugated with biotin (WGA-biotin) (Sigma-Aldrich). After washing four times with PBS, biotin was detected by Chemiluminescent Nucleic Acid Detection Module (Pierce).

Triton X-100-induced autolysis assay

Autolysis assay was performed according to Seidl [27]. The cultures were grown in TSB at 37 °C with shaking to an optical density at 600 nm of approximately 0.8 and harvested through centrifugation. The cells were washed twice with 50 mM Tris–HCl buffer (pH 7.5) and resuspended in a buffer containing 50 mM Tris–HCl (pH 7.5) and 0.1 % Triton X-100. The cells were subsequently incubated at 37 °C with shaking, and the changes in the OD_{600} were measured. The results were normalized to OD_{600} at time zero (OD_0): percentage of initial absorbance at time t = [OD at time t/OD_0] × 100.

Purification and quantification of eDNA

Isolation of eDNA from static biofilms was performed according to previously described methods [14, 28]. Briefly, the cultures incubated overnight in TSB at 37 °C were diluted 200-fold with fresh TSB (containing 0.25 % glucose) supplemented with 3 % NaCl. The diluted cell suspension was inoculated into flat-bottomed 24-well polystyrene plates (Costar 3524, Corning Inc., Corning, NY), containing 1 ml of culture in each well. To assess the impact of DNase I, the cells were grown in medium supplemented with 100 Kuniz units/ml of RNase-free DNase I (Sangon Biotech). After 24 h, the supernatants were discarded, and the unwashed biofilm of each well was

Table 2 Oligonucleotides used in this study

Primers	Sequence (5′–3′)
gyrA RT-S	TTATCGTTATCCGCTTGT
gyrA RT-A	TATTCGTTGCCATACCTAC
leuA RT-S	ATTCGAGTGCCTAGAAATA
leuA RT-A	AGTCGTGCTTACACCAAC
lysA RT-S	GTCCAACAATCTAAACACT
lysA RT-A	CAAAGCCACCACCAAG
RTQ-lytM-f	CATTCGTAGATGCTCAAGGA
RTQ-lytM-r	CTCGCTGTGTAGTCATTGT
RTQ-pta-f	AAAGCGCCAGGTGCTAAATTAC
RTQ-pta-r	CTGGACCAACTGCATCATATCC
rt-rna3-f	GGTTATTAAGTTGGGATGG
rt-rna3-r	GAGTGATTTCAATGGCACA
RTQ-atlE-F	AGCACCAACGGATTAC
RTQ-atlE-R	CATACTCAGCACTGTCT
RT-agrA-f	CCCTCGCAACTGATAATC
RT-agrA-r	CTGCCTAATTTGATACCATT

suspended in 450 µl TE buffer (10 mM Tris·HCl/1 mM ETDA, pH 8.0). The mixture of unwashed biofilms from each well was mixed with 50 µl of 50 µg/ml proteinase K in TE buffer and incubated with shaking at 37 °C for 1 h. After centrifugation, the supernatant containing extracellular material was filtered through 0.22 µm polyethersulfone membranes (PES). Each supernatant (400 µl) was transferred to a tube containing 800 µl of 3 % CTAB buffer (3 % CTAB/150 mM Tris·HCl/30 mM EDTA/2.1 M NaCl, pH 8.0), and incubated at 60 °C for 15 min. The samples were extracted once with 600 µl of phenol/chloroform/isoamyl alcohol (25:24:1) and once with 600 µl chloroform/isoamyl alcohol (24:1). Subsequently, 900 µl of the aqueous phase of each sample was mixed with 108 µl of 5 M ammonium acetate and 605 µl of 100 % (vol/vol) isopropanol and stored at −20 °C for 20 min. The isopropanol-precipitated DNA was collected through centrifugation for 20 min at 4 °C and 18,000 g, washed twice with 75 % (vol/vol) ethanol, air-dried, and dissolved in 500 µl of water. The eDNA was quantified through real-time PCR using the primers listed in Table 2. Quantitative PCR was performed with SYBR *Premix Ex Taq*™ (Takara), according to the manufacturer's instructions in the StepOne™ Real-Time PCR System (Applied Biosystems). Purified genomic DNA of *S. aureus* NCTC8325 at known concentrations was subjected to quantitative PCR with each primer pair to generate a standard curve for calculating the concentration of eDNA in the unknown samples. To account for potential differences in the biomass, the average OD_{600} of each unwashed biofilm was determined and used to calculate the relative OD_{600} of each biofilm with respect to the OD_{600} of the untreated biofilm of the wild-type *S. aureus* (SBY2) (whereby the relative OD_{600} of the SBY2 biofilm = 1). The total eDNA normalized with the relative OD_{600} obtained from the unwashed biofilm was calculated.

RNA isolation

Overnight cultures were inoculated to an optical density of 0.01 into fresh TSB medium. Small-scale RNA was prepared from *S. aureus* cultures at variable growth phases (3–8.5 h). RNA isolation was performed as previously described [29]. *S. aureus* cells were pelleted and lysed in 1 ml of RNAiso (TaKaRa) with 0.7 g of zirconia–silica beads (0.1 mm in diameter) in a high-speed homogenizer (IKA® T25 digital UlTRA-TURRAX®). Total RNA was isolated according to the standard protocol of RNAiso. The isolated RNA was treated with RNase-free DNase I (Takara) to remove the DNA template, and the concentration of RNA was quantified spectrophotometrically at 260 nm.

Quantitative real-time RT-PCR analysis

Real-time RT-PCR was carried out using the PrimeScript™ 1st-strand cDNA Synthesis Kit and SYBR *Premix Ex Taq*™ (Takara), according to the manufacturer's instructions using the oligonucleotides shown in Table 2. Specific primers for each gene were used. Real-time PCR was performed using the StepOne™ Real-Time PCR System (Applied Biosystems). The housekeeping gene *pta* was used as an endogenous control, and the quantity of cDNA measured through real-time PCR was normalized to the abundance of *pta* cDNA [30]. The specificity of the PCR was confirmed using a melting curve of the products. To assess the DNA contamination, each RNA sample was subjected to real-time PCR using SYBR *Premix Ex Taq*™ (Takara).

Results

The bacterial clumping is reduced in the *S. aureus pfs* mutant strain

When *S. aureus* NCTC8325 wild-type strain (SBY2) was grown overnight in TSB medium in glass tubes, the cells clumped together and sank to the bottom of the tube, resulting in a clearance of the medium (Fig. 1a). However, the *pfs* mutant strain (SBY3) culture remained cloudy after overnight growth in TSB medium in glass tubes, indicating that bacterial clumping was defective in the *pfs* mutant strain [27]. This phenotype was also microscopically observed. At the mid-log phase of growth, the wild-type strain culture was filled with clumps of cells, whereas the cells of the *pfs* mutant strain were dispersed (Fig. 1b). This phenotype was restored in the complementation strain (SBY4) (Fig. 1a, b).

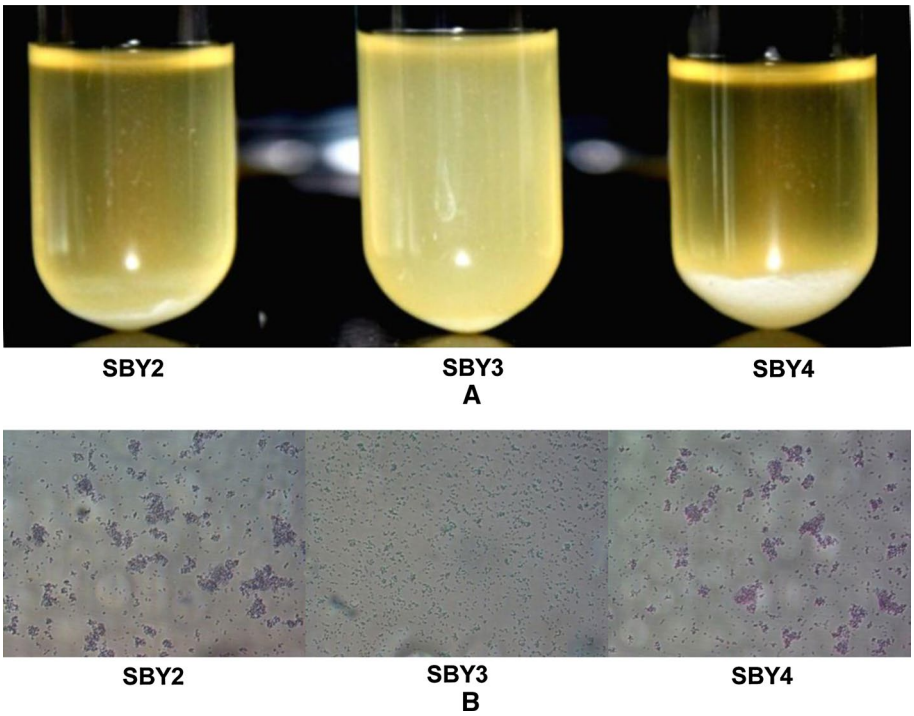

Fig. 1 The bacterial clumping of *S. aureus pfs* mutant strain is reduced. **a** Growth phenotype of the wild-type (SBY2), the *pfs* mutant (SBY3), and complementation (SBY4) strains grown overnight at 37 °C in glass tubes in TSB was compared. The data represent two independent analyses. **b** The clump structure of the log phase cultures of SBY2, SBY3, and SBY4 strains was observed under the view of a microscope. The data represent three independent analyses

The *pfs* mutation reduces *S. aureus* biofilm formation under both static and dynamic flow conditions

The bacterial clumping defect reflects weakened attachment between bacteria [27], which is an important factor in the development of biofilms. We proposed that the reduced intercellular aggregation of the *pfs* mutant strain could lead to reduced biofilm formation. Thus, the biofilm formation of the *pfs* mutant strain (SBY3) was compared with that of the wild-type (SBY2) and the complementation (SBY4) strains under both static and dynamic flow conditions. In the static biofilm assay, SBY3 showed a dramatic reduction in biofilm formation compared with the strains of SBY2 and SBY4 at 24 h after incubation (Fig. 2a). The decreased biofilm formation of the *pfs* mutant strain could not be the consequence of the growth defect, as it has been measured that Pfs is not essential for growth of *S. aureus* under nutrient-rich condition [23].

To better reflect the conditions under which biofilm growth occurs in vivo [31], a once-through continuous culture system was used as previously described [25]. The wild-type (SBY5) and the *pfs* mutant (SBY6) strains constitutively expressing green fluorescent protein (GFP) were used to observe the biofilm structure using confocal laser scanning microscopy (CLSM). For the wild-type and complementation strains, robust biofilms developed as early as 14 h after incubation and increased with time up to 24 h (Fig. 2b; Fig. S1). Conversely, only the sparse attachment of *pfs* mutation cells was visualized (Fig. 2b; Fig. S1).

Biofilm formation proceeds in two distinct developmental phases: the primary attachment of staphylococcal cells to a polystyrene surface, followed by bacterial accumulation in multiple layers [32]. Notably, the reduction in biofilm formation in the *pfs* mutant strain did not reflect a defect in the initial attachment. Similar levels of attached bacteria of the strains SBY2, SBY3, and SBY4 were observed at 60 min post-inoculation on the 24-well plates (Fig. S2). Thus, we concluded that the reduced biofilm formation of the *pfs* mutant strain was a consequence of defects in bacterial accumulation, and the reduced biofilm formation of the *pfs* mutant strain was not related to the factors contributing to the initial attachment of the biofilm formation process, such as FnBPA, FnBPB, ClfA, and ClfB.

The defective biofilm formation in the *pfs* mutant strain was AI-2 independent

As shown in our previous study [23], Pfs is essential for AI-2 production in *S. aureus*. The AI-2 quorum-sensing system has been implicated in the regulation of biofilm formation [33]. Thus, we examined whether the defect in biofilm formation in the *pfs* mutant strain reflected a defect in AI-2 production. The medium was supplemented with the chemically synthesized AI-2 precursor molecule 4,5-dihydroxy-2,3-pentanedione (DPD) at the beginning of biofilm incubation under static conditions at concentrations of 39 or 390 nM, which are the DPD concentrations shown to restore the *luxS* mutant phenotypes well [34]. As shown in Fig. 3a, the addition of AI-2 to the culture medium did not rescue the biofilm formation defect of the *pfs* mutant strain under static conditions. The observed phenotype was also the same under dynamic flow conditions. The

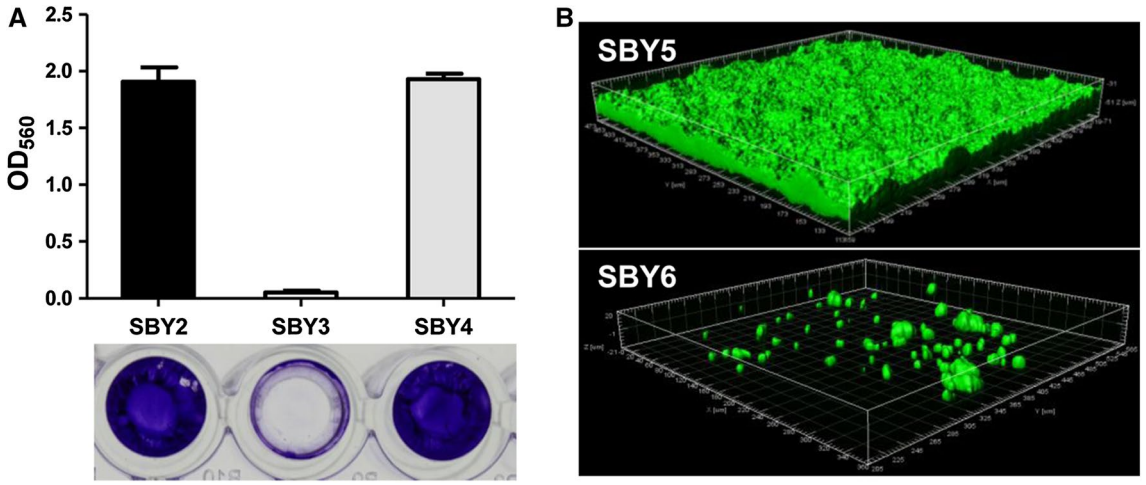

Fig. 2 The *pfs* mutation reduces *S. aureus* biofilm formation. **a** The biofilm formation of the wild-type (SBY2), the *pfs* mutant (SBY3), and the complementation (SBY4) strains was compared at 24 h after incubation under static conditions. The *lower graph* shows crystal violet-stained biofilms attached to wells of microtiter plates. The data represent at least five independent analyses; *error bars* indicate SEM of at least six replicates. **b** The biofilm of the wild-type (SBY5) and the *pfs* mutant (SBY6) strains, with constitutively expressing GFP, was grown in the flow cell system for 24 h, and the fluorescence images were obtained using CLSM (OLYMPUS FV-1000, BX61WI) confocal microscopy with a ×20 OLYMPUS UPLFL objective (NA 0.46). The data represents two independent analyses

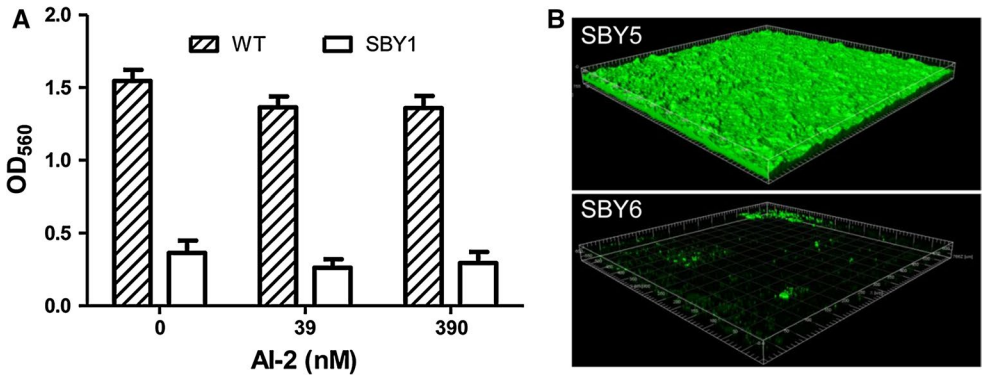

Fig. 3 The reduced biofilm formation of the *pfs* mutant strain is independent of AI-2. **a** The biofilm formation ability of the wild-type (WT) and the *pfs* mutant (SBY1) strains was compared with the addition of 39 or 390 nM AI-2 at the time of inoculation under static conditions for 24 h. **b** The biofilm of the GFP-expressing strains of the wild-type (SBY5) and the *pfs* mutant (SBY6) were grown in the flow cell system for 24 h with the addition of 39 nM AI-2 to the culture medium, and fluorescence images were obtained using CLSM (OLYMPUS FV-1000, BX61WI) confocal microscopy with a ×10 OLYMPUS UPLFL objective (NA 0.3)

addition of 39 nM AI-2 to the culture medium at the beginning of biofilm incubation in the once-through continuous culture system did not rescue the biofilm formation defect of the *pfs* mutant strain (Fig. 3b). These results suggest that the defect of the *pfs* mutant strain in biofilm formation is not because of the disruption of AI-2, consistent with our previous studies showing that the *S. aureus* AI-2 reduces biofilm formation [22].

The reduced biofilm formation of the *pfs* mutant strain is PIA independent

Intercellular adhesion and aggregation of *S. aureus* have mainly been attributed to the production of polysaccharide intercellular adhesion PIA [26, 35]. So, we investigated the transcription of *icaADBC* operon in the wild-type (SBY2), the *pfs* mutant (SBY3), and complementation (SBY4) strains using real-time RT-PCR. As shown in Fig. 4a, we did not observe significant changes in the transcriptional level of the *icaA* after *pfs* knockout. The PIA production was further investigated using the WGA-biotin method. Consistent with the result of real-time PCR, PIA was not changed after *pfs* knockout, neither in the shaking nor the static conditions (Fig. 4b). We also confirmed our results in the strain of SH1000, which forms biofilm in a PIA-independent manner [36]. In our case, the deletion of *pfs* in SH1000 also decreased the biofilm formation

just like in the NCTC8325 strain (Fig. 4c). So, we conclude that the effect of *pfs* on the biofilm formation is PIA independent.

The reduction in biofilm formation of the *pfs* mutant strain is associated with autolysis-dependent eDNA release

The eDNA acts as an adhesive and strengthens the biofilm, which is important for *S. aureus* biofilm formation [13, 16]. Next, we want to know whether the decreased biofilm formation of the *pfs* mutant strain is eDNA dependent or not. The amount of eDNA present in the unwashed 24-h static biofilms was quantified through real-time PCR using three different primer pairs [14]. The total eDNA per relative biomass obtained from unwashed biofilms was determined as previously described [14]. As shown in Fig. 5a, the average amount of eDNA present in the SBY3 biofilm was reduced to 1/10 of that present in the SBY2 biofilm, and the amount of eDNA in the SBY4 biofilm was restored. As a control, the amount of eDNA present in the DNase I-treated biofilms was also determined to eliminate the interference of intracellular DNA. As we can see in Fig. 5a, DNase I treatment reduced the amount of eDNA in the SBY2 biofilm to less than 1/100 of that of the untreated sample. The eDNA amount extracted from the DNase I-treated biofilms of SBY2, SBY3, and SBY4 strains was comparable. On the other side, DNase I treatment totally eliminated the biofilm formation in the three strains (Fig. 5b), implying a critical role for eDNA in *S. aureus* NCTC8325 biofilm development. At the same time, the culture growth was determined through the measurement of the optical density at 600 nm in each well at 24 h after biofilm incubation to ensure that the effect of DNase I on biofilm development did not reflect the effects of this enzyme on bacterial growth (Fig. S3).

Previous studies have demonstrated that eDNA is released through cell lysis [14, 17]. Therefore, we tested whether the decreased eDNA amounts are related to altered autolytic activity. The *pfs* mutant strain showed a reduction in Triton X-100-induced autolysis compared with the wild-type strain. Within 1 h, 56 % and 66 % of the cells from the wild-type (SBY2) and the complementation (SBY4) strains, respectively, were lysed, whereas only 12 % of the cells from the *pfs* mutant strain (SBY3) were lysed (Fig. 5c). These results suggest that the *pfs* mutation might affect *S. aureus* biofilm formation through a reduction in cell lysis and the amount of eDNA present in the biofilm.

The reduced autolysis activity is due to the decreased *atlE* and *lytM* transcription

The major autolysis-related genes of *S. aureus* include *atlE*, *lytM*, *lytH*, *lytA*, *sle1,* and *lytN* as well as some regulators

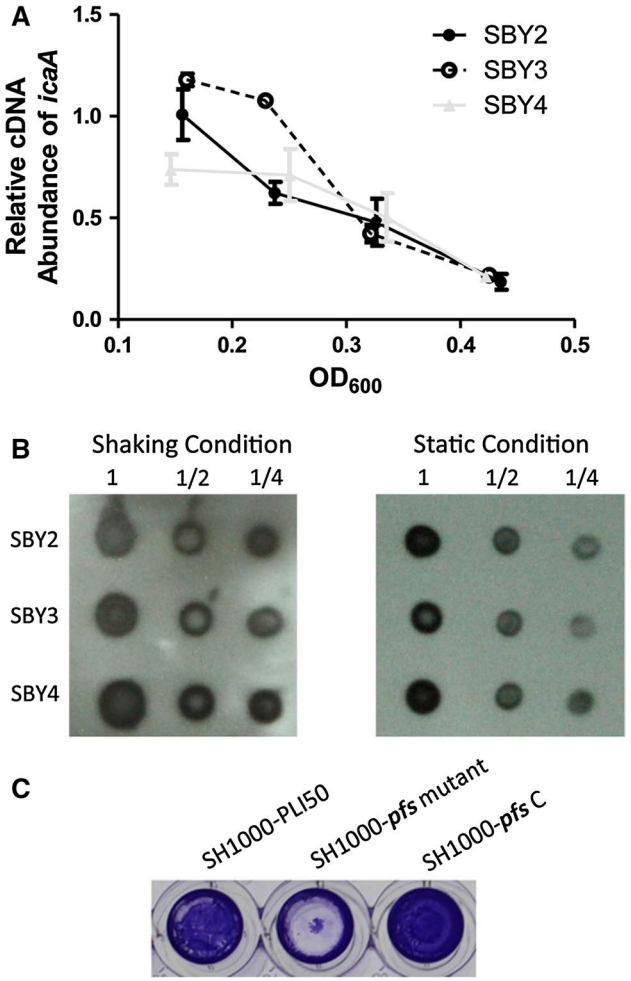

Fig. 4 The reduced biofilm formation of the *pfs* mutant is PIA independent. **a** The transcriptional profile of *icaA* of the *pfs* mutant strain (SBY3) was compared with that of the wild-type (SBY2) and complementation (SBY4) strains. **b** Quantification of PIA of the wild-type (SBY2), the *pfs* mutant strain (SBY3), and complementation (SBY4) strains. PIA was extracted from overnight cultures of each strain, serially diluted, and applied to a nitrocellulose membrane. PIA was detected using WGA-biotin and Chemiluminescent Nucleic Acid Detection Module (Pierce). Numbers at the top indicate times of dilutions. **c** The biofilm formation of the SH1000-pLI50, the SH1000-*pfs* mutant, and the complementation strains SH1000-*pfs* C was compared at 12 h after incubation under static conditions. The biofilms attached to wells of microtiter plates were detected by crystal violet-stained. The data represent at least two independent analyses, and the *error bars* indicate the SEM of three replicates

including *lrgAB, cidAB, arlRS*, *mgrA*, *lytSR*, *sarA*, *sarV*, and *agr* quorum-sensing system [18]. In order to find out how Pfs alters the autolysis activity of *S. aureus*, we tested the transcription levels of these autolysis-related genes using real-time RT-PCR (Fig. 6a; Fig. S4). We observed that the transcription level of *atlE* was reduced in the *pfs* mutant strain at all growth phases (Fig. 6c), and the transcriptional level of *lytM* gene was reduced at the log phase (Fig. 6b). Staphylococcal autolysis is determined to a large

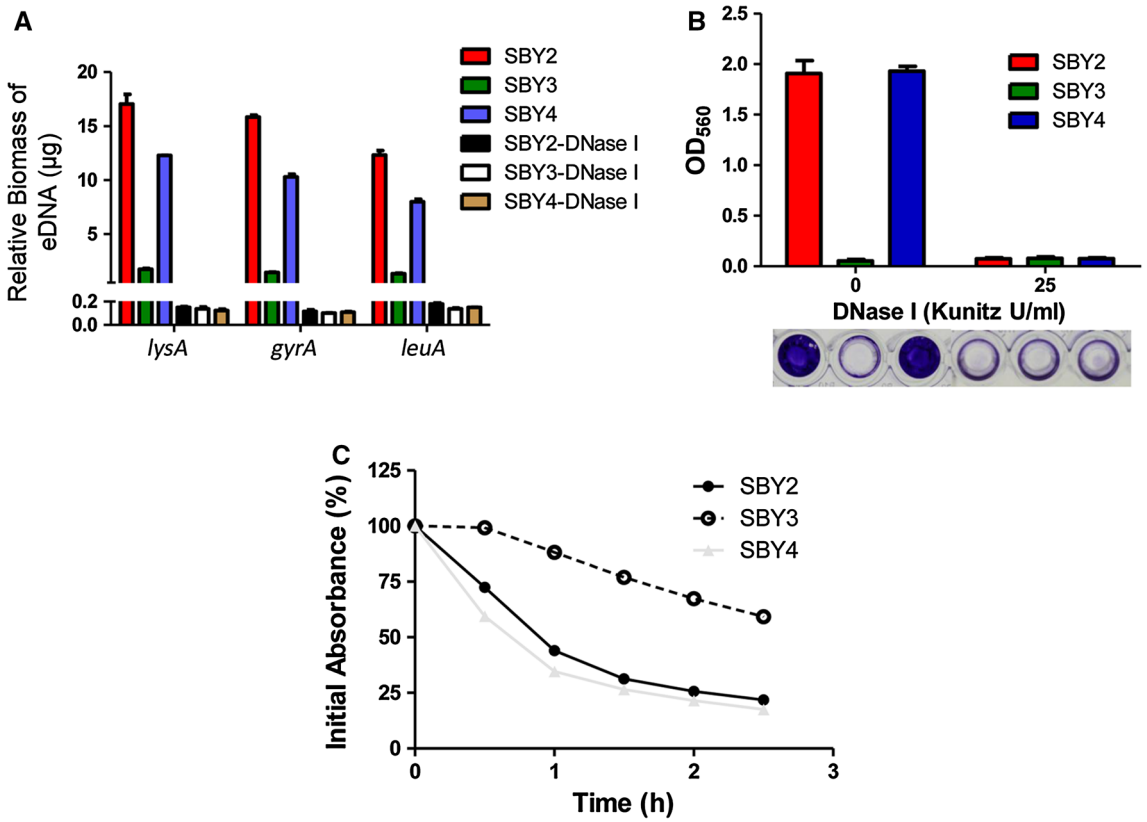

Fig. 5 The reduction in biofilm formation in the *pfs* mutant strain is associated with the reduced autolysis and extracellular DNA (eDNA) content in the biofilm. **a** The amount of eDNA present in the unwashed static biofilm of SBY3 was reduced compared with that present in the SBY2 and SBY4 biofilms. Extracellular DNA was quantified through real-time PCR using primer pairs specific for *gyrA* (gyrase A), *lysA* (diaminopimelate decarboxylase A), and *leuA* (2-isopropylmalate synthase). The values are expressed as total the eDNA per relative biofilm biomass. The data represents two independent analyses; *error bars* indicate SEM of three replicates. **b** eDNA is essential for *S. aureus* NCTC8325 biofilm formation. The addition of DNase I at the time of inoculation eliminated the biofilm formation difference among the wild-type (SBY2), the *pfs* mutant (SBY3), and the complementation (SBY4) strains. The data represent at least three independent analyses, and the *error bars* indicate the SEM of at least five replicates. **c** The *pfs* mutation reduces the autolysis ability of *S. aureus*. Log growth phase cultures of the wild-type (SBY2), the *pfs* mutant (SBY3), and the complementation (SBY4) strains were incubated in a buffer solution containing 50 mM Tris–HCl (pH 7.5) and 0.1 % Triton X-100. The percentage of initial absorbance at 600 nm was determined as an indicator of lysis. The data represent at least three independent analyses, and the *error bars* indicate the SEM of three replicates

extent by the activity of the major autolysin AtlE [37], and *lytM* also acts as another major autolysin gene of *S. aureus*. Thus, we concluded that the reduced transcription of *lytM* and *atlE* might underlie the reduced autolysis observed in the *pfs* mutant strain.

Furthermore, Agr and RNA III were reduced in the *pfs* mutant strain at the log growth phase (Fig. 6d, e). So, *pfs* mutation was constructed in the *agr* null strain RN6911, to investigate whether Agr system is necessary in the biofilm regulation of Pfs. Interestingly, the autolysis and the biofilm formation ability were also decreased in the RN6911-*pfs* mutant (Fig. 7a, b), which suggested that Pfs can promote the biofilm formation through a Agr/RNA III-independent way. The link between Pfs, and *atlE* and *lytM* expression remains to be found.

Discussion

In bacteria, methylthioadenosine/S-adenosylhomocysteine nucleosidase (Pfs) catalyzes the irreversible hydrolytic deadenylation reaction of methylthioadenosine (MTA) [38], S-adenosylhomocysteine (SAH) [39], and 5′-deoxyadenosine (5′dADO) [40], which are the product inhibitors of a broad array of metabolic reactions in the SAM cycle [19]. Until recently, studies concerning Pfs have primarily focused on determining the biochemical properties of this enzyme [41], screening the Pfs inhibitors for the study of their putative antimicrobial activity [42] or identifying the role of Pfs related to the AI-2 signal. In *S. aureus*, the structure of Pfs and the MTA and SAH nucleosidase activity of this enzyme have been determined [43]. And in a previous

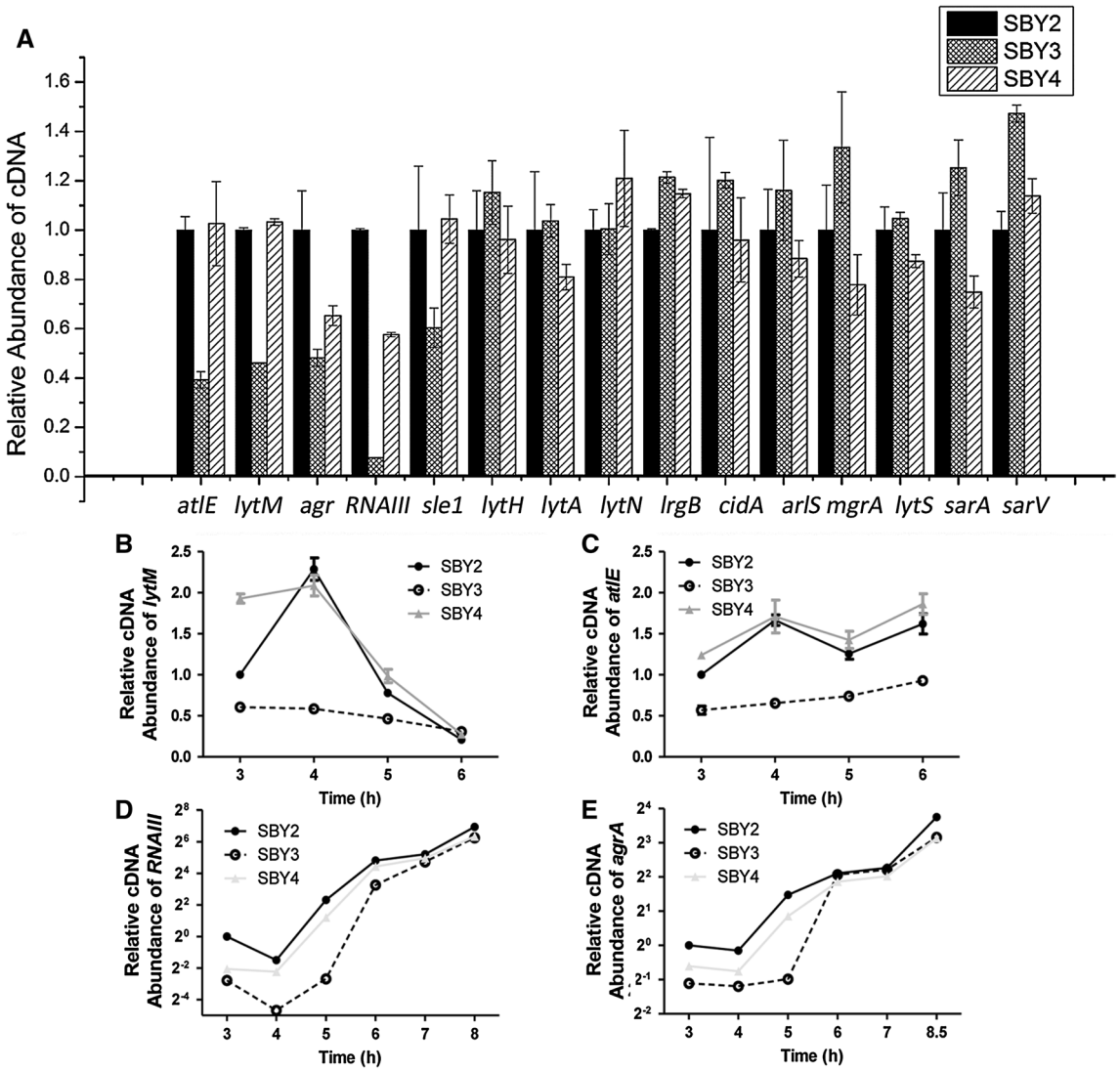

Fig. 6 The *pfs* mutation alters the transcription of the autolysis-related genes in *S. aureus*. **a** The transcription levels of autolysis-related genes of wild-type (SBY2), the *pfs* mutant (SBY3), and the complementation (SBY4) strains were compared using RNA isolated at 4 h. The transcriptional profile of *lytM* (**b**), *atlE* (**c**), *agrA* (**d**), and *RNAIII* (**e**) of the *pfs* mutant strain (SBY3) was compared with that of the wild-type (SBY2) and complementation (SBY4) strains using RNA isolated from the cultures at different growth phases (3–6/8 h). The data represent at least two independent analyses, and the *error bars* indicate the SEM of three replicates

study, we showed that the Pfs of *S. aureus* is essential for the virulence independent of LuxS/AI-2 system [23]. Herein, we revealed that Pfs plays an important role in *S. aureus* biofilm formation.

As Pfs plays an essential role in AI-2 production [23], we determined the dependence of the biofilm formation defect of the *pfs* mutant strain on AI-2. The addition of in vitro-synthesized AI-2 did not restore the biofilm formation of the *pfs* mutant strain under either static or dynamic flow conditions, which suggest that the defect of the *pfs* mutant strain in biofilm formation is not because of the disruption of AI-2. In a previous study, we also showed that *S. aureus* AI-2 quorum-sensing reduces biofilm formation [22]. This means that pfs and AI-2 have opposite effect on biofilm formation. Thus, we conclude that the reduced biofilm formation of the *pfs* mutant strain observed in the present study is AI-2 independent.

In the previous study [23], we demonstrated that the *pfs* mutation reduced the expression of extracellular proteases due to the effects of this mutation on the expression of *sspABC* and *aur* genes. Extracellular proteases, which participate in the detachment step in biofilm formation cycles, inhibit protein-dependent biofilm formation in *S. aureus* [25]. However, we observed that the *pfs* mutation reduced biofilm formation in the *S. aureus* NCTC8325 strain, despite the reduced expression of extracellular proteases.

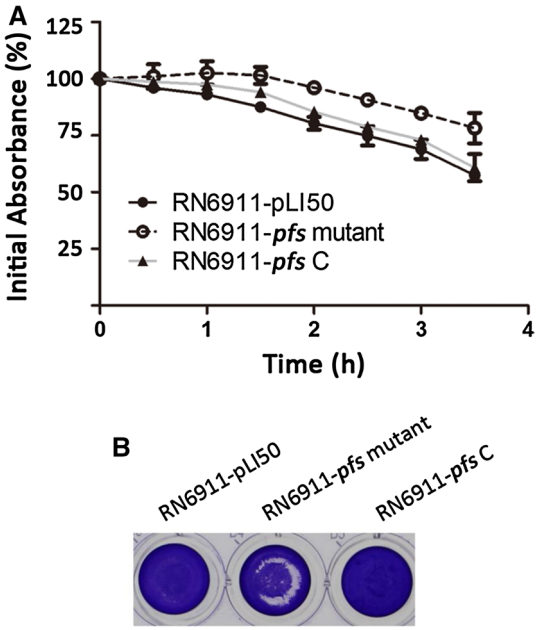

Fig. 7 Pfs can promote the autolysis and biofilm formation in the absence of Agr/RNA III. **a** The *pfs* mutation reduces the autolysis ability of *S. aureus* strain RN6911. Log growth phase cultures of the RN6911-pLI50, the RN6911-*pfs* mutant, and the complementation strains RN6911-*pfs* C were incubated in a buffer solution containing 50 mM Tris–HCl (pH 7.5) and 0.1 % Triton X-100. The percentage of initial absorbance at 600 nm was determined as an indicator of lysis. The data represent at least three independent analyses, and the *error bars* indicate the SEM of three replicates. **b** The biofilm formation of the RN6911-pLI50, the RN6911-*pfs* mutant, and the complementation strains RN6911-*pfs* C was compared at 12 h after incubation under static conditions. The biofilms attached to wells of microtiter plates were detected by crystal violet-stained

This result might reflect variations in the biofilm composition among different strains [15]. As Pozzi C. reported, proteinase K had no significant effect on the biofilm formation in the 8325-4 strain [44]. Biofilm formation is determined through multiple factors. In the present study, we showed that the reduced biofilm formation of the *pfs* mutant strain was associated with reduced autolysis, resulting in the reduced eDNA content in the biofilm. Consistent with previous findings [14, 17], our results showed that eDNA is essential for *S. aureus* biofilm formation, and the impaired biofilm formation associated with reduced autolysis is unrelated to the defects in initial attachment stages of biofilm formation.

We also observed that the reduced autolysis of the *pfs* mutant strain was associated with transcription changes in the autolysis-related genes of *S. aureus* at the log growth phase, including the autolysin genes, *atlE* and *lytM*, and the two divergently transcribed transcripts of *agr* locus, RNAII and RNAIII, which are autolysis-positive regulators. Although it was reported that RNAIII influences the expression of *lytM* [45], we have successfully shown that Pfs inactivation can reduce the autolysis and biofilm formation ability in a genetic background without Agr/RNA III system. This suggests that Pfs can fulfill the regulation in the absence of Agr/RNA III.

In summary, we have shown that mutation of *pfs* has a pleiotropic effect on *S. aureus* with respect to virulence and biofilm formation, highlighting Pfs as a potential anti-infection drug target. Future research is necessary to investigate the mechanism by which mutation of *pfs* has such a global regulatory effect. Considering the conservation of Pfs in a wide variety of bacterial species, it is possible that these roles of Pfs are widely conserved. Our studies may facilitate further investigations into the roles of Pfs in diverse bacterial species.

Acknowledgments This work was supported by the National Natural Science Foundation of China [grants 31070116 and 21304082]. The authors would like to thank the Network on Antimicrobial Resistance in *S. aureus* (NARSA) for providing the bacterial strains.

Conflict of interest The authors declare that they have no conflict of interest.

Ethical standard The authors declare that the experiments comply with the current laws of the country in which they were performed.

References

1. Mainous AG III, Hueston WJ, Everett CJ, Diaz VA (2006) Nasal carriage of *Staphylococcus aureus* and methicillin-resistant *S. aureus* in the United States, 2001–2002. Ann Fam Med 4(2):132–137. doi:10.1370/afm.526
2. Boucher HW, Corey GR (2008) Epidemiology of methicillin-resistant *Staphylococcus aureus*. Clin Infect Dis 46(Suppl 5):S344–S349. doi:10.1086/533590
3. David MZ, Daum RS (2010) Community-associated methicillin-resistant *Staphylococcus aureus*: epidemiology and clinical consequences of an emerging epidemic. Clin Microbiol Rev 23(3):616–687. doi:10.1128/CMR.00081-09
4. Rendueles O, Kaplan JB, Ghigo JM (2013) Antibiofilm polysaccharides. Environ Microbiol 15(2):334–346. doi:10.1111/j.1462-2920.2012.02810.x
5. Donlan RM (2011) Biofilm elimination on intravascular catheters: important considerations for the infectious disease practitioner. Clin Infect Dis 52(8):1038–1045. doi:10.1093/cid/cir077
6. Stoodley P, Sauer K, Davies DG, Costerton JW (2002) Biofilms as complex differentiated communities. Annu Rev Microbiol 56:187–209. doi:10.1146/annurev.micro.56.012302.160705
7. Thomas VC, Thurlow LR, Boyle D, Hancock LE (2008) Regulation of autolysis-dependent extracellular DNA release by *Enterococcus faecalis* extracellular proteases influences biofilm development. J Bacteriol 190(16):5690–5698. doi:10.1128/JB.00314-08
8. Begun J, Gaiani JM, Rohde H, Mack D, Calderwood SB, Ausubel FM, Sifri CD (2007) Staphylococcal biofilm exopolysaccharide protects against *Caenorhabditis elegans* immune defenses. PLoS Pathog 3(4):e57. doi:10.1371/journal.ppat.0030057
9. Thurlow LR, Hanke ML, Fritz T, Angle A, Aldrich A, Williams SH, Engebretsen IL, Bayles KW, Horswill AR, Kielian T (2011) *Staphylococcus aureus* biofilms prevent macrophage

phagocytosis and attenuate inflammation in vivo. J Immunol 186(11):6585–6596. doi:10.4049/jimmunol.1002794
10. Hoyle BD, Costerton JW (1991) Bacterial resistance to antibiotics: the role of biofilms. Prog Drug Res 37:91–105
11. Costerton JW, Stewart PS, Greenberg EP (1999) Bacterial biofilms: a common cause of persistent infections. Science 284(5418):1318–1322
12. Furukawa S, Kuchma SL, O'Toole GA (2006) Keeping their options open: acute versus persistent infections. J Bacteriol 188(4):1211–1217. doi:10.1128/Jb.188.4.1211-1217.2006
13. Gotz F (2002) Staphylococcus and biofilms. Mol Microbiol 43(6):1367–1378. doi:10.1046/j.1365-2958.2002.02827.x
14. Rice KC, Mann EE, Endres JL, Weiss EC, Cassat JE, Smeltzer MS, Bayles KW (2007) The cidA murein hydrolase regulator contributes to DNA release and biofilm development in *Staphylococcus aureus*. Proc Natl Acad Sci USA 104(19):8113–8118. doi:10.1073/pnas.0610226104
15. Trotonda MP, Tamber S, Memmi G, Cheung AL (2008) MgrA represses biofilm formation in *Staphylococcus aureus*. Infect Immun 76(12):5645–5654. doi:10.1128/IAI.00735-08
16. Whitchurch CB, Tolker-Nielsen T, Ragas PC, Mattick JS (2002) Extracellular DNA required for bacterial biofilm formation. Science 295(5559):1487. doi:10.1126/science.295.5559.1487
17. Mann EE, Rice KC, Boles BR, Endres JL, Ranjit D, Chandramohan L, Tsang LH, Smeltzer MS, Horswill AR, Bayles KW (2009) Modulation of eDNA release and degradation affects *Staphylococcus aureus* biofilm maturation. PLoS ONE 4(6):e5822. doi:10.1371/journal.pone.0005822
18. Memmi G, Nair DR, Cheung A (2012) Role of ArlRS in autolysis in methicillin-sensitive and methicillin-resistant *Staphylococcus aureus* strains. J Bacteriol 194(4):759–767. doi:10.1128/JB.06261-11
19. Parveen N, Cornell KA (2011) Methylthioadenosine/S-adenosylhomocysteine nucleosidase, a critical enzyme for bacterial metabolism. Mol Microbiol 79(1):7–20. doi:10.1111/j.1365-2958.2010.07455.x
20. Heurlier K, Vendeville A, Halliday N, Green A, Winzer K, Tang CM, Hardie KR (2009) Growth deficiencies of *Neisseria meningitidis* pfs and luxS mutants are not due to inactivation of quorum sensing. J Bacteriol 191(4):1293–1302. doi:10.1128/JB.01170-08
21. Gutierrez JA, Crowder T, Rinaldo-Matthis A, Ho MC, Almo SC, Schramm VL (2009) Transition state analogs of 5′-methylthioadenosine nucleosidase disrupt quorum sensing. Nat Chem Biol 5(4):251–257. doi:10.1038/nchembio.153
22. Yu D, Zhao L, Xue T, Sun B (2012) *Staphylococcus aureus* autoinducer-2 quorum sensing decreases biofilm formation in an icaR-dependent manner. BMC Microbiol 12:288. doi:10.1186/1471-2180-12-288
23. Bao Y, Li Y, Jiang Q, Zhao L, Xue T, Hu B, Sun B (2013) Methylthioadenosine/S-adenosylhomocysteine nucleosidase (Pfs) of *Staphylococcus aureus* is essential for the virulence independent of LuxS/AI-2 system. Int J Med Microbiol 303(4):190–200. doi:10.1016/j.ijmm.2013.03.004
24. Lim Y, Jana M, Luong TT, Lee CY (2004) Control of glucose- and NaCl-induced biofilm formation by rbf in *Staphylococcus aureus*. J Bacteriol 186(3):722–729
25. Boles BR, Horswill AR (2008) Agr-mediated dispersal of *Staphylococcus aureus* biofilms. PLoS Pathog 4(4):e1000052. doi:10.1371/journal.ppat.1000052
26. Cramton SE, Gerke C, Schnell NF, Nichols WW, Gotz F (1999) The intercellular adhesion (ica) locus is present in *Staphylococcus aureus* and is required for biofilm formation. Infect Immun 67(10):5427–5433
27. Seidl K, Goerke C, Wolz C, Mack D, Berger-Bachi B, Bischoff M (2008) *Staphylococcus aureus* CcpA affects biofilm formation. Infect Immun 76(5):2044–2050. doi:10.1128/IAI.00035-08
28. Wu J, Xi C (2009) Evaluation of different methods for extracting extracellular DNA from the biofilm matrix. Appl Environ Microbiol 75(16):5390–5395. doi:10.1128/AEM.00400-09
29. Wolz C, Goerke C, Landmann R, Zimmerli W, Fluckiger U (2002) Transcription of clumping factor A in attached and unattached *Staphylococcus aureus* in vitro and during device-related infection. Infect Immun 70(6):2758–2762
30. Pereira SF, Henriques AO, Pinho MG, de Lencastre H, Tomasz A (2007) Role of PBP1 in cell division of *Staphylococcus aureus*. J Bacteriol 189(9):3525–3531. doi:10.1128/JB.00044-07
31. Castro SL, Nelman-Gonzalez M, Nickerson CA, Ott CM (2011) Induction of attachment-independent biofilm formation and repression of hfq expression by low-fluid-shear culture of *Staphylococcus aureus*. Appl Environ Microbiol 77(18):6368–6378. doi:10.1128/Aem.00175-11
32. Lou Q, Zhu T, Hu J, Ben HJ, Yang JS, Yu FY, Liu JR, Wu Y, Fischer A, Francois P, Schrenzel J, Qu D (2011) Role of the SaeRS two-component regulatory system in *Staphylococcus epidermidis* autolysis and biofilm formation. BMC Microbiol 11. doi:10.1186/1471-2180-11-146
33. Li J, Attila C, Wang L, Wood TK, Valdes JJ, Bentley WE (2007) Quorum sensing in *Escherichia coli* is signaled by AI-2/LsrR: effects on small RNA and biofilm architecture. J Bacteriol 189(16):6011–6020. doi:10.1128/JB.00014-07
34. Zhao L, Xue T, Shang F, Sun H, Sun B (2010) *Staphylococcus aureus* AI-2 quorum sensing associates with the KdpDE two-component system to regulate capsular polysaccharide synthesis and virulence. Infect Immun 78(8):3506–3515. doi:10.1128/IAI.00131-10
35. Haaber J, Cohn MT, Frees D, Andersen TJ, Ingmer H (2012) Planktonic aggregates of *Staphylococcus aureus* protect against common antibiotics. Plos One 7(7). doi:10.1371/journal.pone.0041075
36. Boles BR, Horswill AR (2008) agr-mediated dispersal of *Staphylococcus aureus* biofilms. Plos Pathog 4 (4). doi:10.1371/journal.ppat.1000052
37. Biswas R, Voggu L, Simon UK, Hentschel P, Thumm G, Gotz F (2006) Activity of the major staphylococcal autolysin Atl. FEMS Microbiol Lett 259(2):260–268. doi:10.1111/j.1574-6968.2006.00281.x
38. Pajula RL, Raina A (1979) Methylthioadenosine, a potent inhibitor of spermine synthase from bovine brain. FEBS Lett 99(2):343–345
39. Simms SA, Subbaramaiah K (1991) The kinetic mechanism of S-adenosyl-L-methionine: glutamylmethyltransferase from *Salmonella typhimurium*. J Biol Chem 266(19):12741–12746
40. Choi-Rhee E, Cronan JE (2005) A nucleosidase required for in vivo function of the S-adenosyl-L-methionine radical enzyme, biotin synthase. Chem Biol 12(5):589–593. doi:10.1016/j.chembiol.2005.04.012
41. Siu KK, Asmus K, Zhang AN, Horvatin C, Li S, Liu T, Moffatt B, Woods VL Jr, Howell PL (2011) Mechanism of substrate specificity in 5′-methylthioadenosine/S-adenosylhomocysteine nucleosidases. J Struct Biol 173(1):86–98. doi:10.1016/j.jsb.2010.06.006
42. Tedder ME, Nie Z, Margosiak S, Chu S, Feher VA, Almassy R, Appelt K, Yager KM (2004) Structure-based design, synthesis, and antimicrobial activity of purine derived SAH/MTA nucleosidase inhibitors. Bioorg Med Chem Lett 14(12):3165–3168. doi:10.1016/j.bmcl.2004.04.006
43. Siu KKW, Lee JE, Smith GD, Horvatin-Mrakovcic C, Howell PL (2008) Structure of *Staphylococcus aureus* 5 '-methylthioadenosine/S-adenosylhomocysteine nucleosidase. Acta Crystallogr F-Struct Biol Cryst Commun 64:343–350. doi:10.1107/s1744309108009275
44. Pozzi C, Waters EM, Rudkin JK, Schaeffer CR, Lohan AJ, Tong P, Loftus BJ, Pier GB, Fey PD, Massey RC, O'Gara JP

(2012) Methicillin resistance alters the biofilm phenotype and attenuates virulence in *Staphylococcus aureus* device-associated infections. PLoS Pathog 8(4):e1002626. doi:10.1371/journal.ppat.1002626

45. Chunhua M, Yu L, Yaping G, Jie D, Qiang L, Xiaorong T, Guang Y (2012) The expression of LytM is down-regulated by RNAIII in *Staphylococcus aureus*. J Basic Microbiol 52(6):636–641. doi:10.1002/jobm.201100426